Electrical properties and near band edge emission of Bi-doped ZnO nanowires

Congkang Xu,[a] Junghwan Chun, and Dong Eon Kim[b]
Department of Physics, Pohang University of Science and Technology, Kyungbuk 790-784, Republic of Korea and Electron Spin Science Center, Pohang University of Science and Technology, Kyungbuk 790-784, Republic of Korea

Ju-Jin Kim
Department of Physics, Chonbuk National University, Jeonju 561–756, Korea

Bonghwan Chon and Taiha Joo
Department of Chemistry, Pohang University of Science and Technology, Kyungbuk 790-784, Republic of Korea

(Received 6 October 2006; accepted 10 December 2006; published online 23 February 2007)

Electrical transport of Bi–ZnO nanowires shows *n*-type semiconducting behavior with a carrier concentration of $\sim 3.5\times10^{8}$ cm^{-1} (2.7×10^{19} cm^{-3}) and an electron mobility of 1.5 cm^2/V s. The carrier concentration is one order of magnitude larger than that of undoped ZnO nanowires, indicating that Bi acts as donor rather than the usual acceptor in ZnO films. The low mobility may be in association with electron scatterings at the boundaries from small size effect of nanowires. Near band edge emission in photoluminescence spectrum of Bi–ZnO nanowires is redshifted relative to undoped ZnO nanorods as a result of enhanced carrier concentration. The donor-acceptor pair transition associated with Bi was also observed at 3.241 eV. © *2007 American Institute of Physics*. [DOI: 10.1063/1.2431715]

Zinc oxide nanowires (NWs) gain ever-increasing interest since they offer a unique opportunity for the fabrication of nanoscale electronic and photonic devices such as resonant tunneling devices, field effect transistors (FETs), and light-emitting devices.[1–3] BiMn-doped ZnO bicrystal nanobelts exhibiting ferromagnetism at room temperature may be applied in spintronics.[4] Ga-doped ZnO NWs can enhance the carrier concentration and subsequently tune their optical properties.[5] The sintering of ZnO with a small amount of Bi dopants gives rise to the formation of a double Schottky barrier, which is known to be important for the fabrication of varistors to sense and limit transient voltage surges.[6–9] Nonetheless, ZnO with a high concentration of Bi may incur a significant surface segregation and/or phase separation, which results in high resistivity and fuzzy carrier types.[10,11] Xiu *et al.*[12] tried to control the Bi content below 0.4% in ZnO films without any phase separation by molecular beam epitaxy (MBE), showing that the carrier concentration decreases significantly because a large amount of Bi induces defect complexes which act as acceptors. ZnO NWs with a small amount of Bi dopants are, therefore, important for nanodevice as well as the understanding of fundamental properties. Furthermore, single-crystalline NWs are suitable for limiting extrinsic effects like secondary phases and achieving low-defect high quality performance. Little is known about the electrical properties and near band edge (NBE) emission of Bi-doped ZnO NWs.

This letter reports the electrical properties and NBE emission of Bi-ZnO NWs. The fabrication of Bi–ZnO NWs was described in a previous report.[13] Figure 1 shows the field emission scanning electron microscopy image of a fabricated Bi–ZnO NW FET and the schematic illustration. To investigate the electrical properties, as-fabricated Bi–ZnO NWs consisting of Zn, O, and Bi with atomic ratios of 48.74, 51.23, and 0.03 were first removed from an oxidized Si substrate by sonicating in ethanol. A heavily doped *n*-type silicon substrate capped with a 300-nm-thick oxide layer (1–10 Ω cm resistivity) was used as a substrate for patterning. Photolithography, successive Ni (100 nm)/Au (50 nm) evaporation, and electron beam lithography were used to pattern the source and drain electrodes and contact a 40-nm-diameter NW with the electrodes. The source-drain electrode distance (channel length) is $L=800$ nm. In this process, both the source and drain electrodes act as alignment marks for electron beam lithography.

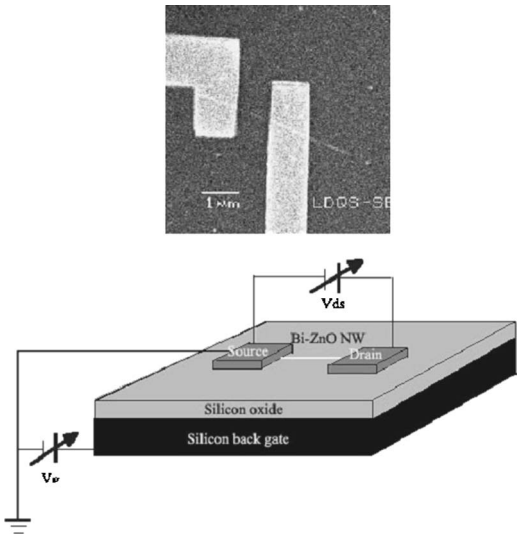

FIG. 1. Scanning electron microscopy image of a Bi–ZnO NW FET with source and drain electrodes.

[a]Electronic mail: ckxu@postech.ac.kr
[b]Author to whom correspondence should be addressed; electronic mail: kimd@postech.ac.kr

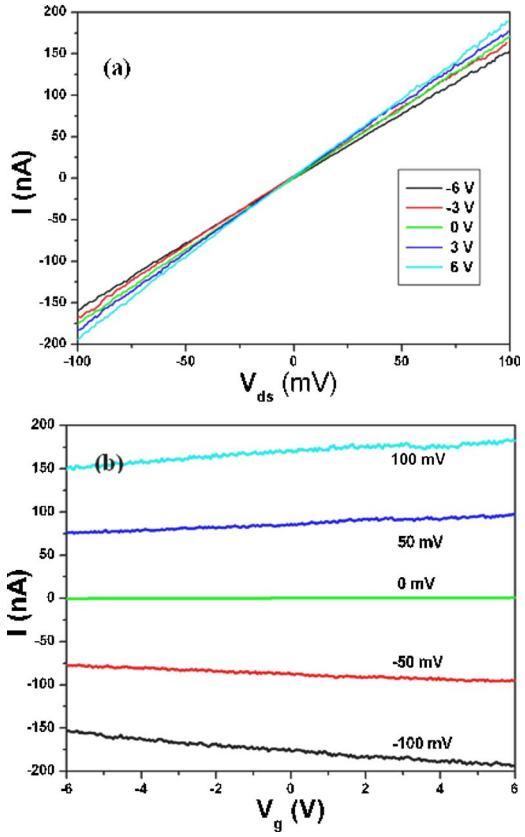

FIG. 2. (Color online) (a) Room-temperature I-V_{ds} curves at different gate voltages. (b) Transconductance of the Bi–ZnO NW FET under $V_{ds}=100$, 50, 0, −50, and −100 mV bias voltages.

Current versus drain-source bias (I-V_{ds}) curves obtained at room temperature under different gate voltages varying from −6 to 6 V with a step of 1.5 V are displayed in Fig. 2(a). The two-terminal I-V_{sd} curves exhibit a linear response, thus indicating that the contacts behave in a practical sense as Ohmic. At a certain V_{sd}, I increases (decreases) with increasingly positive (negative) V_g; that is, the conductance of the nanowire increases (decreases) with positive (negative) gate voltage V_g. This behavior clearly indicates that the ZnO NW FET is an n-channel device. From the I-V_{ds} curves measured at $V_g=0$ and the dimension of the NW, we can get a resistivity (ρ) of about 0.1 Ω cm for the as-obtained Bi–ZnO NW. Figure 2(b) shows transfer characteristic of the NW FET under different biases varying from −100 to +100 mV with a step of 50 mV. The gate response I-V_g curves show again that Bi-doped ZnO nanowire is of n type. The change in current is more than 31 nA by varying the gate voltage from −6 to +6 V. In accordance with Ref. 14, the NW charge carrier concentration n can be denoted by $n=(V_{gt}/e)(2\pi\varepsilon\varepsilon_0/\ln(2h/r))$, where V_{gt} is a threshold gate voltage obtained from transconductance, ε the relative dielectric constant of oxide layer SiO_2, h the gate oxide layer thickness, and r the NW radius. The extrapolation from Fig. 2(b) yields $V_{gt}\approx-56$ V. Using $\varepsilon=3.9$, $h=300$ nm, and $r=20$ nm, the charge carrier concentration is approximately 3.5×10^8 cm^{-1} (or 2.7×10^{19} cm$^{-3}=3.5\times10^8$ cm$^{-1}/\pi r^2$), which is one order of magnitude larger than that of undoped ZnO nanowires.[14] This finding indicates that Bi atoms act as donors unlike the previous reports,[11,12] where Bi atom acts as acceptor. Table I summarizes the electrical data of the undoped and Bi-doped ZnO films/NWs. The undoped ZnO films and NWs have a n-type conductivity with an electron concentration of $\sim10^{18}$ cm^{-3}. The Bi-doped ZnO films and NWs are completely different. The former reveals a significant reduction of electron concentration with a value of 9.1×10^{16} cm^{-3} and Bi showing acceptor feature; the latter exhibits an increase of carrier concentration by a factor of 10 and Bi acting as donors. This discrepancy may arise from the growth conditions and method. In the present study, the method is vapor phase transport, different from MBE and pulsed laser deposition, in which the formation of secondary phase has been observed. Since the as-obtained sample is a high quality single crystal, it can effectively suppress phase separation. The content of Bi is very low as compared with Bi-doped ZnO films[11,12] and the atomic ratio of Bi to Zn observed by energy dispersive x-ray spectroscopy is comparable to the solid solubility (~0.06 mole %) of Bi_2O_3 in ZnO.[15] The secondary phase is, therefore, not expected to be developed. Both x-ray diffractometer patterns and high-resolution transmission electron microscopy image prove that there is no secondary phase in Bi-doped ZnO NWs, indicating that Bi has been doped into ZnO.[13] It is generally difficult for Bi^{3+} to be incorporated into the Zn^{2+} site of ZnO if the mixture of Bi_2O_3 with ZnO powders is sintered since the radius (0.11 nm) and valence of Bi^{3+} are not comparable to those of Zn^{2+} (0.07 nm). Nonetheless, iodide used in the present work has an advantage of low dissociation temperature, which allows Zn atoms to be mixed with BiI_3/Bi on an atomic scale along with the oxidization reaction being minimized. When Bi substitutes Zn site to form Bi_{Zn}, Bi_{Zn}

TABLE I. Electrical properties of undoped and Bi-doped ZnO films/NW.

Sample	Bi dopant type	Conduction type	Carrier concentration (cm^{-3})	Mobility (cm^2/V s)	Resistivity (Ω cm)
Undoped ZnO film[a]	···	n	2.7×10^{18}	7.4	0.3
Bi-doped ZnO film[a]	p type (acceptor)	n	9.1×10^{16}	15.9	4.3
Undoped ZnO NW[b]	···	n	1.4×10^{18}	17.2	0.2
Bi-doped ZnO NW[c]	n type (donor)	n	2.7×10^{19}	1.5	0.1

[a]Reference 12.
[b]Reference 14.
[c]This work.

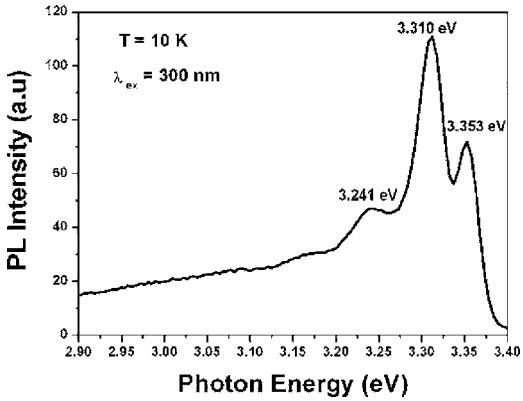

FIG. 3. PL spectra of Bi–ZnO NWs at 10 K excited by 300 nm laser light.

itself is a donor, thus releasing electrons. An enhancement in carrier concentration indicates that Bi_{Zn} is predominant over other point defects such as Bi_{Zn}–Zn vacancies (V_{Zn})–interstitials (O_i) or $Bi_{Zn}-2V_{Zn}$ defect complexes inducing shallow acceptor states in terms of the first principles.[16,17] The mobility (μ_e) in the back-gated Bi–ZnO NW FETs can be further estimated from the transconductance of the FET: $\mu_e = g_m L \ln(2h/r)/\pi\varepsilon\varepsilon_0 V_{sd}$, where $g_m = dI_{ds}/dV_g$. Using $g_m = 2.5\times10^{-9}$ A/V and $V_{ds}=100$ mV, the value is estimated to be 1.5 $cm^2/V\,s$. The mobility of electrons is one order of magnitude lower than that of undoped ZnO NW and Bi-doped ZnO films, as shown in Table I. When the diameter of NWs is less than the mean free path of electron carriers (~100 nm) at room temperature,[18] electron scatterings at the boundaries become significant.[19] Since the diameter (~40 nm) of Bi-doped ZnO NWs is much less than 100 nm, the significant electron scatterings at boundaries are expected and would affect the electrical transport. By studying ZnO:Al films, Ellmer and Vollweiler[20] found that the mobility could decrease significantly due to electrical grain boundaries for $n<3\times10^{20}$ cm^{-3}. In this work, Bi is similar to Al acting as a donor in ZnO, and the carrier concentration of Bi-doped ZnO NWs is below 3×10^{20} cm^{-3}. It is therefore believed that the carrier transport is limited due to electron scatterings at the boundaries.

To validate the presence of Bi dopant in ZnO NWs, low temperature photoluminescence (PL) measurements were carried out with a 300 nm excitation source. Figure 3 shows PL spectrum of Bi-doped ZnO NWs at 10 K, which contains three emission lines at 3.241, 3.310, and 3.353 eV around NBE. Based on peak assignments in Refs. 21 and 22, the slightly weaker well-resolved line at 3.353 eV was identified as donor bound (D^oX) and the pronounced line at 3.310 eV as longitudinal optical phonon replica of the ground state exciton. In ZnO single crystal nanorods at 10 K,[23] donor-bound exciton (D^o, X) lines appeared at 3.360 and 3.364 eV. NBE emission of Bi-doped ZnO NWs is redshifted relative to that of undoped ZnO nanorods. The reduction of NBE transition energy is believed to be the result of the doping-induced band gap renormalization effect due to enhanced carrier concentration.[24] It is noteworthy that, different from the undoped ZnO, a Bi-doped ZnO NW emits another emission at about 3.241 eV. In effect, the emissions with similar photon energies reported in N-doped (3.216 eV),[25] P-doped (3.241 eV),[26] and Bi-doped (3.222 eV) (Ref. 12) ZnO films were shown to be donor-acceptor pair (DAP) transitions. Accordingly, the line at 3.241 eV in Bi-doped ZnO NWs can be assigned to the DAP transition associated with Bi dopants, which further give evidence that Bi exists in ZnO NWs.

In summary, electrical transport of Bi-ZnO NWs shows n-type semiconductor behavior with a carrier concentration of $\sim3.5\times10^8$ cm^{-1}(2.7×10^{19} cm^{-3}) and an electron mobility of 1.5 $cm^2/V\,s$. The carrier concentration is one order of magnitude larger than that of undoped ZnO NWs, indicating that Bi acts as a donor rather than the usual acceptor as in ZnO films. The low mobility may be in association with enhanced electron scatterings at the grain boundaries due to the small size of NWs. NBE emission in photoluminescence spectrum of Bi-ZnO NWs is red-shifted relative to that of undoped ZnO nanorods as a result of enhanced carrier concentration. The DAP transition associated with Bi was observed at 3.241 eV, indicating the existence of Bi dopant.

This work was partially supported by electron Spin Science Center (eSSC), National Research Laboratory (NRL) projects funded by Korean Science and Engineering Foundation (KOSEF), and Brain Korea (BK) 21.

[1] M. T. Bjork, B. J. Ohlsson, C. Thelander, A. I. Persson, K. Deppert, L. R. Wallenberg, and L. Samuelson, Appl. Phys. Lett. **81**, 4458 (2002).
[2] M. S. Gudiksen, L. J. Lauhon, J. Wang, D. C. Smith, and C. M. Lieber, Nature (London) **415**, 617 (2002).
[3] Y. Wu, R. Fan, and P. Yang, Nano Lett. **2**, 83 (2002).
[4] C. Xu, J. Chun, K. Rho, H. J. Lee, Y. H. Jeong, D. E. Kim, B. Chon, S. Hong, and T. Joo, Appl. Phys. Lett. **89**, 093117 (2006).
[5] C. Xu, M. Kim, J. Chun, and D. E. Kim, Appl. Phys. Lett. **86**, 133107 (2005).
[6] D. R. Clarke, J. Am. Ceram. Soc. **82**, 485 (1999).
[7] S. Tanaka, C. Akita, N. Ohashi, J. Kawai, H. Haneda, and J. Tanaka, J. Solid State Chem. **105**, 36 (1993).
[8] J. R. Lee, Y. M. Chiang, and G. Ceder, Acta Mater. **45**, 1247 (1997).
[9] D. R. Clarke, J. Appl. Phys. **49**, 2407 (1978).
[10] A. Gulino and I. Fragala, Chem. Mater. **14**, 116 (2002).
[11] J. R. Duclere, R. O. Haire, A. Meaney, K. Johnston, I. Reid, G. Tobin, J. P. Mosnier, M. G. Viry, E. Mcglynn, and M. O. Henry, J. Mater. Sci. **16**, 421 (2005).
[12] F. X. Xiu, L. J. Mandalapu, Z. Yang, J. L. Liu, G. F. Liu, and J. A. Yamoff, Appl. Phys. Lett. **89**, 052103 (2006).
[13] C. Xu, K. Rho, J. Chun, and D. E. Kim, Appl. Phys. Lett. **87**, 253104 (2005).
[14] Z. Fan, D. Wang, P. Chang, W. Tseng, and J. Lu, Appl. Phys. Lett. **85**, 5923 (2004).
[15] J. Luo and Y. M. Chiang, J. Eur. Ceram. Soc. **19**, 697 (1990).
[16] J. M. Carlsson, H. S. Domingos, P. D. Bristowe, and B. Hellsing, Phys. Rev. Lett. **91**, 165506 (2003).
[17] S. Limpijumnong, S. B. Zhang, S. H. Wei, and C. H. Park, Phys. Rev. Lett. **92**, 155504 (2004).
[18] S. B. Cronin, Y. M. Lin, O. Rabin, M. R. Black, J. Y. Ying, M. S. Dresselhaus, P. L. Gai, J. P. Minet, and J.-P. Issi, Nanotechnology **13**, 653 (2002).
[19] A. F. Mayadas and M. Shatzkes, Phys. Rev. B **1**, 1382 (1970).
[20] K. Ellmer and G. Vollweiler, Thin Solid Films **496**, 104 (2006).
[21] J. Gutowski, N. Presser, and I. Broser, Phys. Rev. B **38**, 9746 (1988).
[22] C. Xu, K. Rho, J. Chun, and D. E. Kim, Nanotechnology **17**, 60 (2006).
[23] W. I. Park, Y. H. Jun, S. W. Jung, and C. Yi, Appl. Phys. Lett. **82**, 964 (2003).
[24] J. D. Ye, S. L. Gu, S. M. Zhu, S. M. Liu, Y. D. Zhang, R. Zhang, and Y. Shi, Appl. Phys. Lett. **86**, 192111 (2005).
[25] L. J. Wang and N. C. Giles, Appl. Phys. Lett. **84**, 3049 (2004).
[26] D. K. Hwang, H. S. Kim, J. H. Lim, J. Y. Oh, J. H. Yang, S. J. Park, K. K. Kim, D. C. Look, and Y. S. Park, Appl. Phys. Lett. **86**, 151917 (2005).